

Some Achievements in Neutron Crystallography

B. T. M. WILLIS

Chemical Crystallography Laboratory, 9 Parks Road, Oxford OX1 3PD, England.

E-mail: bertram.willis@chemcryst.ox.ac.uk

(Received 20 January 1998; accepted 8 April 1998)

Abstract

In this article, some results are described in a few areas of crystallography in which the methods of neutron scattering have played a major role. Four areas are selected: the determination of magnetic structures, high-resolution powder diffraction, crystallography at high pressure, and the measurement of phonon-dispersion relations. In each case, the results are considered in the context of complementary information provided by synchrotron X-ray studies.

1. Introduction

With the availability in the 1940s of thermal neutron fluxes from nuclear reactors, it was apparent that the technique of neutron scattering could be used for studying the structure and dynamical properties of materials. The importance of neutron scattering was underlined much later by the award of the 1994 Nobel Prize for Physics to Clifford Shull 'for the development of the neutron diffraction technique' and to Bertram Brockhouse 'for pioneering contributions to the development of neutron scattering'.

B. T. M. Willis gained an honours degree in Physics from the University of Cambridge in 1948 and a PhD from the University of London in 1951. From 1951 to 1953, he was a member of the research staff of the General Electric Company, London, and from 1954 to 1984 a research scientist at the Atomic Energy Research Laboratory, Harwell, England. Since 1985, he has been a Senior Research Fellow at the Chemical Crystallography Laboratory, University of Oxford. He is a professorial Fellow of the University of Wales and has been a Visiting Professor in Physics in Denmark, India, Switzerland and Japan. He has published numerous papers on the theory and practice of neutron scattering, and has co-authored several books. Since 1966, he has organized at Harwell, and later at Oxford, regular biennial Summer Schools on Neutron Scattering. His work on behalf of the International Union of Crystallography includes being Chairman of the Commission on Neutron Diffraction (1984–1987) and a Co-editor of Acta Crystallographica (1980–1990).

The contributions made by neutron scattering to the characterization of materials are described in recent reviews (Harrison & Willis, 1994; Harrison, 1995), conference proceedings (Funahashi *et al.*, 1995; Bauer *et al.*, 1997), and books (Higgins & Benoît, 1994; Furrer, 1995; Schoenborn & Knott, 1996). In this article, we shall restrict our attention to results from four areas of crystallography, *viz* the determination of magnetic structures, high-resolution powder diffraction, crystallography at high pressure and the measurement of phonon-dispersion relations. The results will be chosen to illustrate not only progress in these four areas over the past 50 years but also the complementarity of such studies with related work employing synchrotron X-ray scattering.

2. Magnetism

Neutron scattering provides the most incisive method for determining magnetic structures. An early neutron success was the experimental proof by Shull & Smart (1949) of the antiferromagnetism predicted by Néel (1948). Shull & Smart found that at 80 K the moments of the manganese ions in MnO are aligned in equal numbers, parallel and antiparallel, along each of the cubic axes, giving rise to a magnetic cell that is double the size of the chemical cell. Since then, a large number of more complicated magnetic structures have been studied. For example, the rare-earth metals have magnetic structures in which the magnetic moments are arrayed in a 'helifan', which is intermediate between a helix and a fan (Cowley & Bates, 1988; Cowley *et al.*, 1994; Simpson *et al.*, 1996). Different helifan structures are obtained by changing the temperature or by varying the applied magnetic field, and these structures may have commensurate regions of spin separated by discommensurations or 'spin slips' (Jensen & Mackintosh, 1990).

In recent years, one of the most interesting problems in magnetism has been the measurement and interpretation of the extremely large magnetoresistance of certain manganese oxides related to the perovskite LaMnO₃ (see Aeppli *et al.*, 1997). A material whose electrical resistance changes in response to a magnetic field is said to show magnetoresistance (MR). Thus,

permalloy, an alloy of nickel and iron which is used in reading magnetic hard discs, shows a small MR of 3%. Thin films of Fe and Cr display a much larger change in MR on applying a field: the effect is so large that it has been given a new name – *giant* magnetoresistance (GMR). An even larger change, a reduction of up to 1000-fold, was then observed in bulk phases of the perovskites $(\text{La}_{1-x}\text{Ca}_x)\text{MnO}_3$. This extraordinary effect, whose physical origin is quite different from the GMR observed in layered compounds, has called for a yet more emphatic name – *colossal* magnetoresistance (CMR). The CMR in $(\text{La}_{1-x}\text{Ca}_x)\text{MnO}_3$ is very sensitive to the precise composition and magnetic structure. In $\text{La}^{3+}\text{Mn}^{3+}\text{O}_3$ at one end of the series ($x = 0$), the manganese is entirely trivalent; as we proceed through the range, Mn^{3+} is continuously replaced by Mn^{4+} until we arrive at the other end ($x = 1$), where the composition is $\text{Ca}^{2+}\text{Mn}^{4+}\text{O}_3$ and the manganese is entirely tetravalent. For the composition range $0.2 < x < 0.5$, CMR materials undergo a paramagnetic to ferromagnetic transition on cooling, which is accompanied by a sharp drop in resistivity. The transition temperature is raised in a magnetic field, resulting in a colossal magnetoresistance near this temperature.

This surge of interest in the properties of the rare-earth manganate perovskites has refocused attention on the pioneering neutron-diffraction measurements carried out four decades ago by Wollan & Koehler (1955), who examined the series of perovskite compounds $(\text{La}_{1-x}\text{Ca}_x)\text{MnO}_3$, supplementing their neutron data with X-ray studies of the distortions from ideal cubic symmetry. Fig. 1 illustrates some of the antiferromagnetic structures found by Wollan & Koehler. The open and closed circles of the structure elements in this figure represent equal numbers of parallel and antiparallel spins, which are arranged in magnetic cells requiring a doubling of the chemical cell along one or more of the cube edges. LaMnO_3 has the *A* structure, with manganese atoms lying in ferromagnetic [100] sheets and with spins oppositely directed in adjacent sheets. CaMnO_3 has the *G* structure with each of the three sets of (100) sheets of atoms containing an equal number of oppositely directed spins. Thus, whereas the magnetic cell in *A* is doubled in one direction only compared with the chemical cell, it is doubled in all three directions in the *G* structure. The

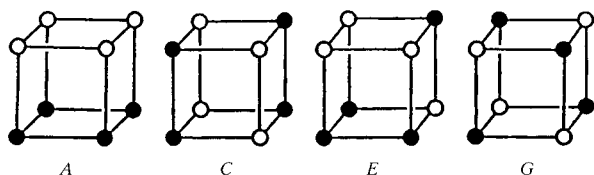


Fig. 1. Some of the structure elements found in the series of perovskite-type compounds $(\text{La}_{1-x}\text{Ca}_x)\text{MnO}_3$. The solid and open circles represent oppositely directed spins. (After Wollan & Koehler, 1955.)

structure of the *C* type, observed at a composition of about $x = 0.75$, requires doubling of the cell in two directions. In the region $x = 0.50$, there is a more complicated antiferromagnetic phase, illustrated in Fig. 2. The magnetic unit cell, which repeats the chemical cell four times in two directions and twice in the third direction, is derived by stacking the *C* and *E* cubes in Fig. 1 in an ordered arrangement of Mn^{3+} and Mn^{4+} ions.

The magnetic transitions in $(\text{La}_{0.75}\text{Ca}_{0.25})\text{MnO}_3$ and $(\text{La}_{0.50}\text{Ca}_{0.50})\text{MnO}_3$ have been studied by Radaelli *et al.* (1995) by powder diffraction employing both neutron and synchrotron X-ray diffraction. On cooling below the transition temperature, sharp changes were observed in the orthorhombic lattice parameters. Furthermore, broad peaks appeared in the transition region which could not be indexed with a single unit cell. The peak profiles were fitted by assuming four domains, each of *Pbnm* symmetry and possessing slightly different cell parameters. These subtleties were not revealed in the earlier studies, thus emphasizing how the contribution of neutron scattering has increased with improvements in resolution. The study by Battle *et al.* (1990) of the crystal and magnetic structures of the anion-deficient perovskite $\text{Sr}_2\text{LaFe}_3\text{O}_8$ is another example of the joint use of neutron and synchrotron X-ray diffraction data. X-ray magnetic scattering cross sections are orders of magnitude weaker than neutron cross sections, but X-ray intensities can be magnified using *resonant* scattering (McWhan, 1994). Resonant enhancement scattering is especially useful for compounds of elements such as gadolinium, which have an extremely large neutron absorption cross section (de Costa *et al.*, 1996).

The polarized neutron technique is employed with single crystals to determine the spatial distribution of unpaired spins in the unit cell. These experiments usually require large magnetic fields and low temperatures to induce polarization of the spins. By measuring a sufficiently large number of magnetic structure factors, the magnetization density is derived by a Fourier analysis with the structure factors as coefficients. The procedure was first applied by Shull & Yamada (1962) to obtain the spin density of iron, and the results were interpreted in terms of the relative occupation of e_g and t_{2g} orbitals. A good modern example of the method is the measurement of the spin density in an organic ferromagnet by Zheludev *et al.* (1995), where the analysis showed that the unpaired electron is delocalized over several atoms and can act as a magnetic bridge in designing other molecular compounds with different magnetic properties.

3. Powder diffraction

Many materials are not available in a form suitable for structural characterization by X-ray single-crystal methods, and this has stimulated progress in the *ab initio*

determination of structures from powder diffraction measurements. It is worth recording that 50 years ago Zachariasen published a remarkable series of papers in the first volume of *Acta Crystallographica*, describing the determination of the crystal structures of compounds of thorium, of uranium and of transuranic elements. These compounds were only available in powder form and the structures were found from X-ray powder patterns.

Cernik *et al.* (1991) have solved the crystal structure of cimetidine, $C_{10}H_{16}N_6S$, from synchrotron X-ray powder data: 33 atoms in the asymmetric unit were located of which half were H atoms. By harnessing the combined powers of high-resolution synchrotron X-ray and neutron powder techniques, Morris *et al.* (1994) have solved the structure of $La_3Ti_5Al_{15}O_{37}$, which has 60 atoms in the asymmetric unit. The ability to resolve adjacent powder lines is ultimately limited by their intrinsic width, and for this reason it may not be possible to solve more complex structures in this way. The strong point of synchrotron radiation is high resolution, and solving reasonably complex structures of up to 40 atoms is now essentially routine; neutron powder diffraction comes into its own in the subsequent refinement process. Indeed, most studies of neutron powder diffraction have concerned the refinement of known structures, usually by Rietveld analysis, and in the following paragraphs we shall refer to a few of the more recent examples.

Neutron powder diffraction has proved to be of fundamental importance for determining the structures

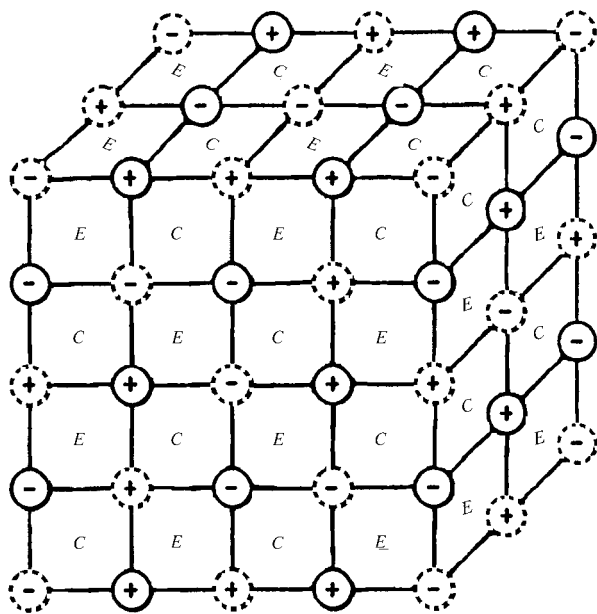


Fig. 2. The antiferromagnetic structure of the 'charge-ordered' phase $La_{0.5}Ca_{0.5}MnO_3$ showing the manganese atoms only. The broken circles are Mn^{3+} and the closed circles are Mn^{4+} . The + and - signs refer to oppositely directed spins. (After Wollan & Koehler, 1955.)

of high-temperature oxide superconductors for which single crystals are not available (see Hewat, 1990, 1992; Kamiyama *et al.*, 1994). In these superconductors, X-rays are scattered principally by the heavy metal atoms (such as barium or bismuth or the rare earths), whereas thermal neutrons are scattered just as strongly by oxygen, which is the atom of most significance in understanding the superconducting properties. There have been many studies of $YBa_2Cu_3O_{7-\delta}$ and of related compounds with yttrium replaced by rare-earth ions (see Beyers & Shaw, 1989, and the review by Radaelli, 1998). The primary aim of these investigations was to determine the total oxygen content and the distribution of oxygen in the unit cell. Capponi *et al.* (1987) examined $YBa_2Cu_3O_{7-\delta}$ between 5 and 300 K by neutron powder diffraction and showed that the oxygen vacancies are ordered, in contradiction to earlier X-ray work. The work of Kaldis *et al.* (1989) on $YBa_2Cu_4O_8$ links with the high-pressure studies described in the next section. This 80 K superconductor has a structure similar to that of the 123 superconductor $YBa_2Cu_3O_7$ but with the Cu–O chains doubled along the c axis. By applying a moderate pressure of 1 GPa (10 kbar), the superconducting transition temperature is increased by 5 K, and this represents one of the largest known changes of T_c with pressure for high- T_c compounds (Bucher *et al.*, 1989). Using the D2B diffractometer at the High Flux Reactor of the ILL, Grenoble, Kaldis *et al.* (1989) carried out measurements as a function of both temperature and pressure. The principal structural change as the pressure increases is in the position of the oxygen atoms bridging Cu–O planes with Cu–O chains, and this suggests that the increase in T_c is associated with an increase in the number of electron holes in the Cu–O planes. The D2B instrument has been employed also in studying bismuth-oxide-type superconductors; here the structure is based on a distorted perovskite cell in which small tilts of the BiO_6 octahedra occur about the tetragonal c axis (Kazakov *et al.*, 1997).

Extensive powder diffraction measurements have been carried out on crystalline C_{60} , using a pulsed neutron source: with this source, the powder pattern can be observed to a value of $|\mathbf{Q}| = 4\pi \sin \theta / \lambda$ (where \mathbf{Q} is the scattering vector) as high as 45 \AA^{-1} (see Axe *et al.*, 1994). C_{60} is the most stable of the carbon cage molecules, collectively known as the fullerenes (Kroto, 1997). It is a highly symmetric molecule, which contains 60 atoms arranged at the vertices of a truncated icosahedron consisting of 12 pentagons and 20 hexagons (see Fig. 3). The C–C bonds are of two types: the '6:6' bonds fusing two hexagons and the '6:5' bonds fusing a hexagon and a pentagon. The C_{60} units pack together at all temperatures from liquid-helium to room temperature as crystals with cubic symmetry.

At room temperature, the space group of C_{60} is $Fm\bar{3}m$. This space group is inconsistent with the icosahedral molecular symmetry, and so some kind of

statistical disorder must take place to achieve the higher crystal symmetry. Neutron diffuse scattering and inelastic scattering experiments indicate that the molecules undergo orientational disorder while their centres of mass occupy the sites of a face-centred cubic lattice (Copley *et al.*, 1992). Single-crystal synchrotron X-ray measurements of Chow *et al.* (1992) showed that there is a slight dependence of the scattering on the direction of \mathbf{Q} , suggesting that some molecular orientations are more probable than others. These authors carried out a surface harmonic expansion of the scattering density and derived the high-order cubic harmonic coefficients giving the extent of the departure from spherical symmetry. An analysis by David *et al.* (1993) of neutron powder data in this disordered phase also showed deviations from isotropic scattering, and the high-order coefficients were in broad agreement with those derived by Chow *et al.* from the more precise single-crystal measurements. (The powder data gave understandably poorer statistics and, because reflections sharing the same $|\mathbf{Q}|$, such as 333 and 511, occur at the same $\sin \theta/\lambda$, this overlap reduces the possibility of resolving directional information in a powder pattern.)

David *et al.* (1993) extended their structural investigation to low temperatures, using the high-resolution powder diffractometer (HRPD) at the pulsed neutron source of the ISIS facility. HRPD has exceptionally good resolution on account of the long neutron flight path, 100 m, and the very high scattering angle, close to 180° . Over 100 powder patterns were recorded in 2 K steps between 10 K and room temperature, and they were analysed by the Rietveld method at each temperature to give the crystal structure, including the determination of the lattice parameters to a few parts per million. David

et al. (1993) showed that, in addition to the first-order phase change at 260 K identified earlier by synchrotron X-ray diffraction (Heiney, 1992), there is also a more subtle orientational glass transition at 86 K. Thus, three cubic phases have been identified. In phase I, above 260 K, C_{60} is a *plastic crystal* in the space group $Fm\bar{3}m$, with the molecules constantly reorienting. In phase III, below 86 K, this reorientational motion is frozen out and the space-group symmetry is reduced to $Pa\bar{3}$. The intermediate phase II, between 86 and 260 K, also belongs to the space group $Pa\bar{3}$ but there is restricted motion of the molecules involving hopping between two distinct orientations, which are energetically nearly equivalent. These two orientations are such that the short 6:6 bonds of one molecule point towards the pentagons (ground state) or hexagons (excited state) of adjacent molecules. By fitting the temperature dependence of the lattice parameter to various thermodynamic functions, David *et al.* (1993) determined the energy difference for the two orientations and their fractional occupations throughout the temperature range of phase II. As the temperature is lowered from 260 K, more and more molecules assume the energetically favorable pentagon orientation; below the 'glass transition' at 86 K, the kinetics of reorientation becomes extremely slow and any residual disorder remains frozen.

Other notable studies by neutron powder diffraction include the measurement of the preferred orientation in bones and its relation to bone fracture (Bacon & Goodship, 1991), and the determination of the structure of zirconium tungstate as a function of temperature (David *et al.*, 1998). ZrW_2O_8 is remarkable in possessing a negative thermal expansion over its entire temperature range from absolute zero to its decomposition temperature around 1050 K. The crystal structure of ZrW_2O_8 contains corner-sharing ZrO_6 octahedra and WO_4 tetrahedra which make up the framework lattice. Data were collected on HRPD in 5 min runs at intervals of 2 K up to 550 K, and a Rietveld refinement at each temperature gave the lattice constant and the anisotropic displacement parameters (ADPs) of the oxygen atoms. The analysis of these ADPs indicated that the polyhedra vibrate as rigid units with very pronounced libration. The librational correction to the bond length causes an effective bond shortening which in turn leads to a negative thermal expansion (see Fig. 4).

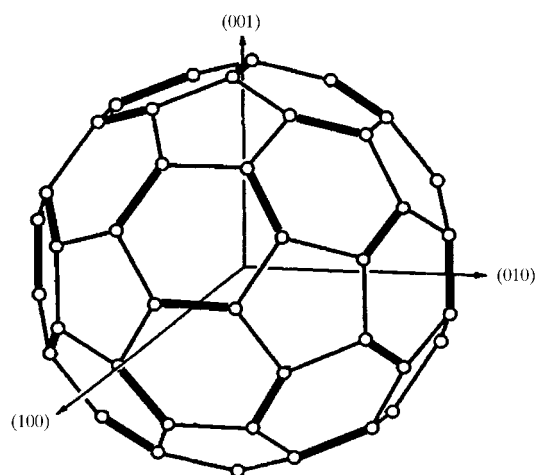


Fig. 3. The C_{60} molecule showing the 6:6 bonds as heavier lines and the 6:5 bonds as lighter lines. These bond lengths have been measured at 295 and 20 K by pulsed-neutron powder diffraction: they are essentially the same at the two temperatures and are 1.400 Å for the electron-rich 6:6 bond and 1.440 Å for the electron-poor 6:5 bond. (After Soper *et al.*, 1992.)

4. Crystallography at high pressure

The solar system contains over 90% by mass of hydrogenous molecules such as H_2 , H_2O , NH_3 and CH_4 under pressures in excess of 10 GPa. Inside the earth itself, a large amount of water exists under pressure as H_2O or as OH^- in minerals of the crust and upper mantle. According to Finger *et al.* (1989), the water now on the surface could have been stored in minerals deep

in the mantle, and has been released gradually through volcanic eruptions. Neutron powder diffraction is a powerful method of probing the structural properties at high pressure of these low-*Z* materials. Although the substitution of hydrogen by deuterium is unnecessary in single-crystal diffraction, it is customary to use deuterated materials for powder studies whenever possible, as this greatly reduces the spin-incoherent scattering in the background of the neutron pattern.

X-ray studies of low-*Z* materials have been carried out at pressures well above 10 GPa using cells with single-crystal diamond anvils (DACs), but the relatively low flux of neutron sources implies large sample volumes and restricts the employment of DACs. For many years, no techniques were available to take samples of sufficiently large volume above 3 GPa, and so earlier studies (Brugger *et al.*, 1967; Kuhs *et al.*, 1984; Jorgensen & Worlton, 1985; Stokes *et al.*, 1993) were confined to this pressure range. Angle-dispersive measurements using diamond-anvil cells have been reported by Russian workers (Glazkov *et al.*, 1989; Goncharenko *et al.*, 1996) at much higher pressures, but the samples were minute (less than 0.1 mm³) and gave acute intensity problems which precluded a full structure analysis.

A dramatic improvement has taken place in recent years in the field of high-pressure neutron diffraction, arising from the development of a novel high-pressure cell by the Paris–Edinburgh group (Besson *et al.*, 1992, 1994; Nelmes, Loveday, Wilson, Besson, Klotz, Hamel & Hull, 1993). This cell (the P–E cell) permits neutron studies up to 10 GPa with a sample volume of 100 mm³ and up to 30 GPa with a volume of 35 mm³. Its use brings neutron work much nearer the pressure range accessible to synchrotron X-rays. The pressure in the P–E cell is generated between opposed anvils of tungsten carbide or sintered diamonds, using a piston driven by

high-pressure oil or helium gas. The cell is designed for operation at a pulsed spallation source, and by adopting the neutron time-of-flight method with a fixed scattering-angle it is possible to reduce the apertures required for the incident and diffracted beams and to screen out spurious scattering from the bulky pressure cell.

At least 12 crystalline phases of ice are known to exist as a function of pressure and temperature, but above 2.1 GPa only two phases are known, ice VII and ice VIII. Ice VII is a cubic disordered phase and ice VIII is its ordered counterpart; these two phases have been examined in their deuterated forms by powder neutron diffraction (Besson & Nelmes, 1995). In ice VIII there is an unexpectedly small variation of the covalent O–D bond length with pressure up to 10 GPa, suggesting that the principal effect of pressure is to reduce the O–D force constants without changing the bond length significantly (Nelmes, Loveday, Wilson, Besson, Pruzan, Klotz, Hamel & Hull, 1993). This is the first experiment where the covalent bond of a hydrogen (deuterium) atom has been measured over a sufficient pressure range to yield its pressure coefficient.

The P–E cell has also been used successfully to study compounds that are gases at ambient pressure and temperature. Samples of deuterated ammonia, hydrogen sulfide and methane have been loaded in the cell at low temperature and under pressure, and examined by powder diffraction as a function of pressure using the PEARL instrument at the ISIS pulsed neutron source (Klotz *et al.*, 1995).

Solid ammonia is a constituent of the outer planets of the solar system. At a pressure of 1 GPa, the gas condenses to a close-packed phase with orientationally disordered molecules arranged on a face-centred cubic lattice. At 4 GPa, this phase transforms to ‘phase IV’, and an X-ray study by Otto *et al.* (1989) indicated that phase IV persists up to pressures of 50 GPa and beyond. Otto *et al.* (1989) suggested that the phase is hexagonal close-packed, space group $P6_3/mmc$, but the full structure was solved later by neutron diffraction (Loveday *et al.*, 1996) in the orthorhombic space group $P2_12_12_1$. The X-ray measurements were extended to much higher pressures than the neutron work, and we see again the value of complementary neutron/X-ray studies.

Hydrogen sulfide, which is a weakly bonded analogue of water, undergoes a phase transition of the disordered f.c.c. phase I at ambient pressure to the partially ordered phase I’ at 9 GPa. The structure of I’ has been solved by Loveday & Nelmes (1998) using combined synchrotron X-ray and neutron data.

5. Phonons

With improvements in the measurement of Bragg intensities, the ‘anisotropic displacement parameters’, which arise from the vibrations of the atoms and are

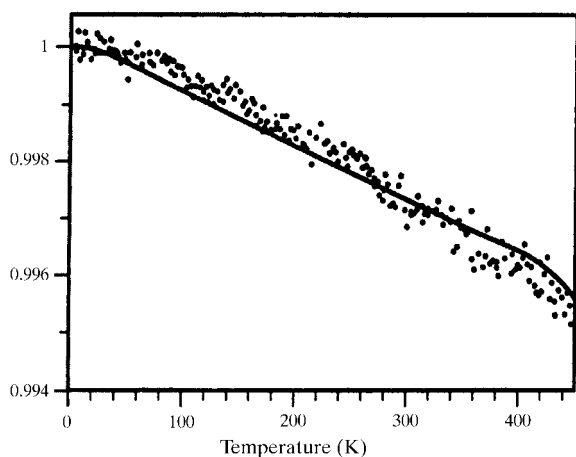


Fig. 4. Fractional decrease with temperature of lattice spacing (full line) and fractional reduction in Zr–O bond length (dotted points) due to correlated librational motion. (After David *et al.*, 1998.)

derived routinely in a structure analysis, assume greater significance. In the case of zirconium tungstate cited above, the measured ADPs were necessary in correcting the bond lengths for the influence of librational motion and for explaining the negative thermal expansion. Nevertheless, to obtain detailed information about lattice vibrations, it is necessary to make measurements of the thermal diffuse scattering (TDS) in reciprocal space away from the Bragg points. The scattering can be regarded as elastic Bragg scattering in the frame of the crystal, in which an individual phonon displaces the atoms from their equilibrium positions with a sinusoidal variation determined by the phonon wavevector. Following Brockhouse's invention of the triple-axis neutron spectrometer in the late 1950s, inelastic neutron scattering has proved to be the most powerful method of studying the lattice dynamics of crystalline solids. The method gives a direct measurement of the dispersion

curves relating the frequency and wavevector of the phonons. These curves can then be analysed in terms of the force constants describing the various atomic interactions in the crystal (see Willis, 1996).

The dispersion curves of aluminium were the first to be determined by neutron scattering (Brockhouse & Stewart, 1958). To date nearly all dispersion relations have been obtained in this way. The book by Bilz & Kress (1979) gives a 'phonon atlas' containing the phonon-dispersion curves of more than a hundred crystals, including half the elements, a large number of diatomic compounds, and rather fewer molecular crystals. Noteworthy examples of recent neutron work are the measurement of the transverse acoustic phonon frequencies of Ge at pressures up to 9.7 GPa (Klotz *et al.*, 1997) and the study by Pintschovius *et al.* (1989) of single-crystal La_2NiO_4 . La_2NiO_4 is isostructural with the high-temperature superconductor $(\text{La, Sr})_2\text{CuO}_4$ and all

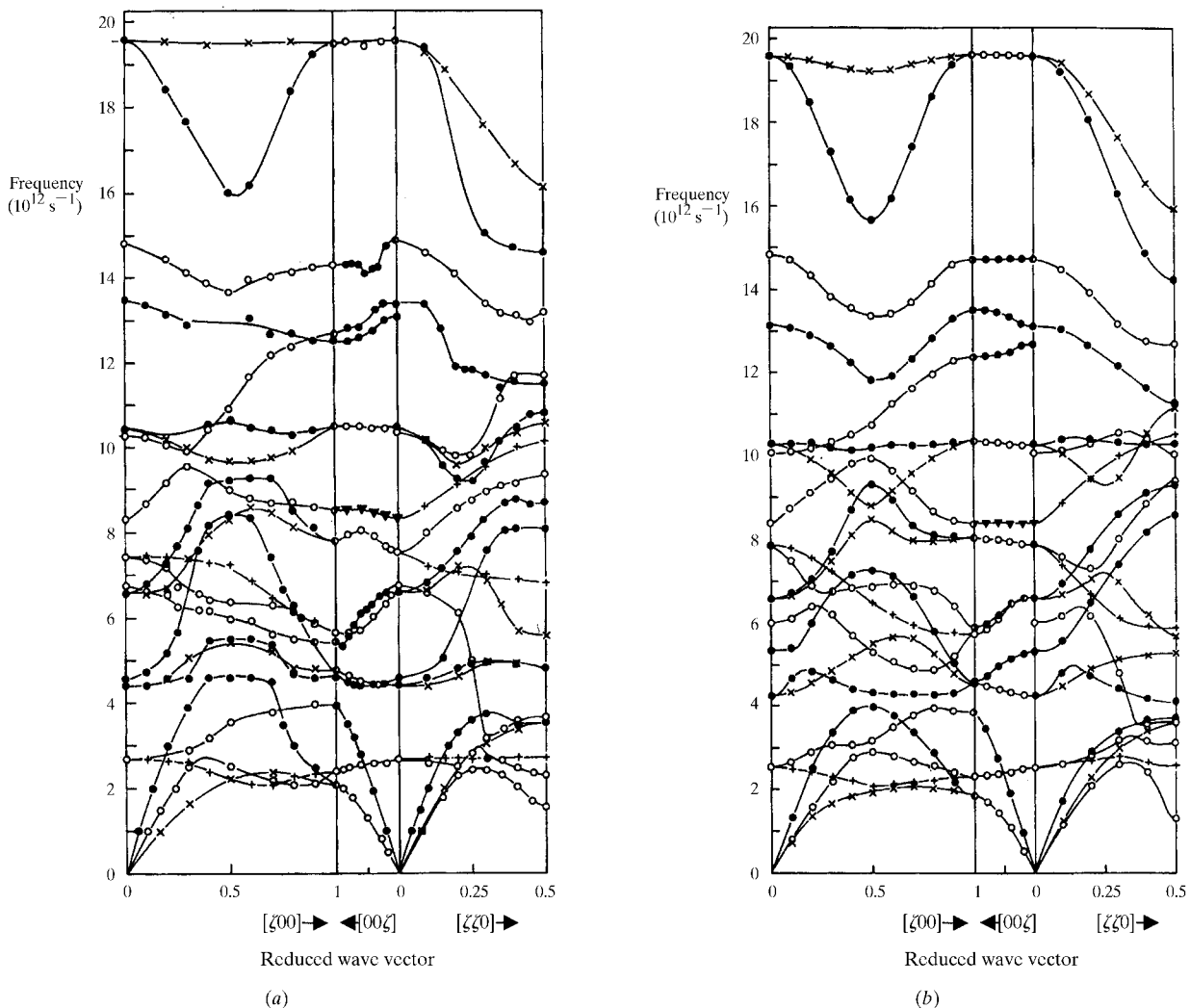


Fig. 5. (a) Experimentally determined and (b) calculated phonon-dispersion curves of Li_2NiO_4 . (After Pintschovius *et al.*, 1989.)

branches of the dispersion curves of La_2NiO_4 were determined in the main symmetry directions [100], [110] and [111]. There are 7 atoms in the unit cell and hence 21 branches for each crystallographic direction. These measurements are shown in Fig. 5(a) together with the calculated dispersion curves, Fig. 5(b). A complicated force field was necessary in these calculations to describe the essential features of the observed curves, and yet some discrepancies still remained. Modelling the dispersion relations of simple ionic solids, such as AgCl or AgBr (Fischer *et al.*, 1972), is difficult enough and so it is perhaps not surprising that these experiments are no longer fashionable. At a recent international conference on neutron scattering (Bauer *et al.*, 1997), two or three papers only, out of a total exceeding 600, reported measurements of dispersion curves.

Phonon-dispersion curves have also been measured by inelastic X-ray scattering. Using synchrotron X-rays and a specially constructed spectrometer with an energy resolution $\Delta E/E$ of 10^{-6} , Dorner *et al.* (1987) determined the dispersion curves in beryllium for the longitudinal-acoustic and longitudinal-optic modes propagating in the [001] direction. In spite of the intensity loss demanded by this exceptionally high resolution, single crystals of mm^3 size can be examined with X-rays, whereas neutrons require cm^3 samples. Thus, X-rays come into their own for small crystals and for those containing boron, cadmium or the rare earths, which are elements with an unacceptably high absorption cross section for thermal neutrons.

There is one feature of the one-phonon scattering of neutrons for which there is no parallel with X-rays. Under certain conditions, the thermal diffuse scattering of slower-than-sound neutrons is forbidden in some regions of reciprocal space and allowed in others. The determination of the sharp boundary between these two regions leads to estimates of the sound velocities in the crystal. These sound velocities can be used subsequently in evaluating the TDS correction to the Bragg intensities. The theory of this effect is described by Popa & Willis (1994, 1997), and the corresponding neutron scattering experiments by Carlile & Willis (1989) and Carlile *et al.* (1992).

6. Conclusions

In a survey of this kind, it is impossible to do justice to all areas of neutron scattering that are of relevance to crystallography. An arbitrary selection has been made of four such areas: magnetism, powder diffraction, high-pressure crystallography and crystal excitations. No reference has been made to structural studies of polymers (see Higgins & Benoît, 1994), to the study of thin films and interfaces by neutron specular reflection (reviewed by Lu *et al.*, 1996) or to dynamical diffraction by perfect crystals. Perhaps the most serious omission is the neutron work on biological macromolecules, a field

that holds great promise following recent advances in the techniques of data collection (Helliwell, 1997). Niimura *et al.* (1997) describe a pioneering study of lysozyme to 2 Å resolution, using Laue diffraction with a wide band of wavelengths and employing a cylindrical image plate detector encircling the protein crystal sample. The protein concanavalin A has also been examined by this new system of data collection (Habash *et al.*, 1997) along with a parallel study of the protein to 0.94 Å resolution with synchrotron radiation (Deacon *et al.*, 1997). Neutron scattering permits determination of hydrogen-deuterium exchange, which can be vital to the understanding of protein activity.

References

- Aeppli, G., Hayden, S. & Perring, T. (1997). *Phys. World*, **10**, No. 12, 33–37.
- Axe, J. D., Moss, S. C. & Neumann, D. A. (1994). *Solid State Phys.* **48**, 135–212.
- Bacon, G. E. & Goodship, A. E. (1991). *J. Anat.* **179**, 15–22.
- Battle, P. D., Gibb, T. C. & Lightfoot, P. (1990). *J. Solid State Chem.* **84**, 237–244.
- Bauer, G. S., Böni, P. & Fischer, P. (1997). Editors. *Proceedings of First European Conference on Neutron Scattering. Physica (Utrecht)*, **B234–236**, 1–1258.
- Besson, J. M. & Nelmes, R. J. (1995). *Physica (Utrecht)*, **B213&214**, 31–36.
- Besson, J. M., Nelmes, R. J., Hamel, G., Loveday, J. S., Weill, G. & Hull, S. (1992). *Physica (Utrecht)*, **B180&181**, 907–910.
- Besson, J. M., Pruzan, Ph., Klotz, S., Hamel, G., Silvi, B., Nelmes, R. J., Loveday, J. S., Wilson, R. M. & Hull, S. (1994). *Phys. Rev. B*, **49** 12540–12550.
- Beyers, R. & Shaw, T. M. (1989). *Solid State Phys.* **42**, 135–212.
- Bilz, R. & Kress, W. (1979). *Phonon Dispersion Relations in Insulators*. Berlin: Springer-Verlag.
- Brockhouse, B. N. & Stewart, A. T. (1958). *Rev. Mod. Phys.* **30**, 236–249.
- Brugger, R. M., Bennion, R. B. & Worlton, T. G. (1967). *Phys. Lett.* **24A**, 714–717.
- Bucher, B., Karpinski, J., Kaldis, E. & Wachter, P. (1989). *Physica (Utrecht)*, **C157**, 478–482.
- Capponi, J. J., Chaillout, C., Hewat, A. W., Lejay, P., Marezio, M., Nguyen, N., Raveau, B., Soubeyroux, J. L., Tholence, J. L. & Tournier, R. (1987). *Europhys. Lett.* **3**, 1301–1307.
- Carlile, C. J., Keen, D. A., Wilson, C. C. & Willis, B. T. M. (1992). *Acta Cryst.* **A48**, 826–829.
- Carlile, C. J. & Willis, B. T. M. (1989). *Acta Cryst.* **A45**, 708–715.
- Cernik, R. J., Cheetham, A. K., Prout, C. K., Watkin, D. J., Wilkinson, A. P. & Willis, B. T. M. (1991). *J. Appl. Cryst.* **24**, 222–226.
- Chow, P. C., Jiang, X., Reiter, G., Woehner, P., Moss, S. C., Axe, J. D., Hanson, J. C., McMullan, R. K., Meng, R. L. & Chu, C. W. (1992). *Phys. Rev. B*, **69**, 2943–2946.
- Copley, J. R. D., Neumann, D. A., Cappelletti, R. L. & Kamitakahara, W. A. (1992). *J. Phys. Chem. Solids*, **53**, 1353–1371.
- Costa, M. M. R. de, Almeida, M. J. M., Nuttall, W. J., Stirling, W. G., Tang, C. C., Forsyth, J. B. & Cooper, M. J. (1996). *J. Phys. Condens. Matter*, **8**, 2425–2435.

- Cowley, R. A. & Bates, S. (1988). *J. Phys. C*, **21**, 4113–4124.
- Cowley, R. A., Ward, R. C. C., Wells, M. R., Matsuda, M. & Sternlieb, B. (1994). *J. Phys. Condens. Matter*, **6**, 2985–2998.
- David, W. I. F., Evans, J. S. O. & Sleight, A. W. (1998). *Acta Cryst. B*. Submitted.
- David, W. I. F., Ibberson, R. M. & Matsuo, T. (1993). *Proc. R. Soc. London Ser. A*, **442**, 129–146.
- Deacon, A., Gleichmann, T., Kalb, A. J., Price, H., Raftery, J., Bradbrook, G., Yariv, J. & Helliwell, J. R. (1997). *J. Chem. Soc. Faraday Trans.* **93**, 4305–4312.
- Dorner, B., Burkel, E., Illini, Th. & Peisl, J. (1987). *Z. Phys.* **B69**, 179–183.
- Finger, L. W., Ko, J., Hazen, R. M., Gasparik, T., Hemley, R. J., Prewitt, C. T. & Weidner, D. J. (1989). *Nature (London)*, **341**, 140–142.
- Fischer, K., Bilz, H., Haberhorn, R. & Weber, W. (1972). *Phys. Status Solidi*, **B54**, 285–294.
- Funahashi, S., Katano, S. & Robinson, R. A. (1995). Editors. *Proceedings of Yamada Conference on Neutron Scattering. Physica (Utrecht)*, **B213&214**, 1–1064.
- Furrer, A. (1995). Editor. *Magnetic Neutron Scattering*. Singapore: World Scientific.
- Glazkov, V. P., Goncharenko, I. N., Irodova, V. A., Somenkov, V. A. & Shilstein, S. Sh. (1989). *Z. Phys. Chem.* **163**, 509–514.
- Goncharenko, I. N., Mignot, J.-M. & Mirebeau, I. (1996). *Neutron News*, **7**, No. 3, 29–31.
- Habash, J., Raftery, J., Weisgerber, S., Cassetta, A., Lehmann, M. S., Hoghoj, P., Wilkinson, C., Campbell, J. W. & Helliwell, J. R. (1997). *J. Chem. Soc. Faraday Trans.* **93**, 4313–4317.
- Harrison, A. (1995). *Annual Reports on the Progress of Chemistry*, Vol. 92, Section A, pp. 405–431. London: Royal Society of Chemistry.
- Harrison, A. & Wills, A. S. (1994). *Annual Reports on the Progress of Chemistry*, Vol. 91, Section A, pp. 437–466. London: Royal Society of Chemistry.
- Heiney, P. A. (1992). *J. Phys. Chem. Solids*, **53**, 1333–1352.
- Helliwell, J. R. (1997). *Nature Struct. Biol.* **4**, 874–876.
- Hewat, A. W. (1990). *Neutron News*, **1**, No. 1, 28–34.
- Hewat, A. W. (1992). *Nuclear Sci. Eng.* **110**, 408–416.
- Higgins, J. S. & Benoît, H. C. (1994). *Polymers and Neutron Scattering*. Oxford University Press.
- Jensen, J. & Mackintosh, A. R. (1990). *Phys. Rev. Lett.* **64**, 2699–2702.
- Jorgensen, J. D. & Worlton, T. G. (1985). *J. Chem. Phys.* **83**, 329–333.
- Kaldis, E., Fischer, P., Hewat, A. W., Hewat, E., Karpinski, J. & Rusiecki, S. (1989). *Physica (Utrecht)*, **C159**, 668–680.
- Kamiyama, T., Izumi, F., Takahashi, H., Jorgensen, J. D., Dabrowski, B., Hitterman, R. L., Hinks, D. G., Shaked, H., Mason, T. O. & Seabaugh, M. (1994). *Physica (Utrecht)*, **C229**, 377–388.
- Kazakov, S. M., Chaillout, C., Bordet, P., Capponi, J. J., Nunez-Regueiro, M., Rysak, A., Tholence, J. L., Radaelli, P. G., Putlin, S. N. & Antipov, E. V. (1997). *Nature (London)*, **390**, 148–150.
- Klotz, S., Besson, J. M., Braden, M., Karch, K., Pavone, P., Strauch, D. & Marshall, W. G. (1997). *Phys. Rev. Lett.* **79**, 1313–1316.
- Klotz, S., Gauthier, M., Besson, J. M., Hamel, G., Nelmes, R. J., Loveday, J. S., Wilson, R. M. & Marshall, W. G. (1995). *Appl. Phys. Lett.* **67**, 1188–1190.
- Kroto, H. (1997). *Rev. Mod. Phys.* **69**, 703–722.
- Kuhs, W. F., Finney, J. L., Vettier, C. & Bliss, D. V. (1984). *J. Chem. Phys.* **81**, 3612–3623.
- Loveday, J. S. & Nelmes, R. J. (1998). To be published.
- Loveday, J. S., Nelmes, R. J., Marshall, W. G., Besson, J. M., Klotz, S. & Hamel, G. (1996). *Phys. Rev. Lett.* **76**, 74–77.
- Lu, J. R., Lee, E. M. & Thomas, R. K. (1996). *Acta Cryst.* **A52**, 11–41.
- McWhan, D. B. (1994). *J. Synchrotron Rad.* **1**, 83–90.
- Morris, R. E., Owen, J. J., Stalick, J. K. & Cheetham, A. K. (1994). *J. Solid State Chem.* **111**, 52–57.
- Néel, L. (1948). *Ann. Phys. (Paris)*, Ser. 12, **3**, 137–198.
- Nelmes, R. J., Loveday, J. S., Wilson, R. M., Besson, J. M., Klotz, S., Hamel, G. & Hull, S. (1993). *Trans. Am. Crystallogr. Assoc.* **29**, 19–27.
- Nelmes, R. J., Loveday, J. S., Wilson, R. M., Besson, J. M., Pruzan, Ph., Klotz, S., Hamel, G. & Hull, S. (1993). *Phys. Rev. Lett.* **71**, 1192–1195.
- Niimura, N., Minezaki, Y., Nonaka, T., Castagna, J.-C., Cipriani, F., Hoghoj, P., Lehmann, M. S. & Wilkinson, C. (1997). *Nature Struct. Biol.* **4**, 909–914.
- Otto, J. W., Porter, R. F. & Ruoff, A. L. (1989). *J. Phys. Chem. Solids*, **50**, 171–175.
- Pintschovius, L., Bassat, J. M., Gervais, F., Chevrier, G., Reichardt, W. & Gompf, F. (1989). *Phys. Rev. B*, **40**, 2229–2238.
- Popa, N. C. & Willis, B. T. M. (1994). *Acta Cryst.* **A50**, 57–63.
- Popa, N. C. & Willis, B. T. M. (1997). *Acta Cryst.* **A53**, 537–545.
- Radaelli, P. G. (1998). In *Physics and Chemistry of Materials with Low-Dimensional Structures*, edited by A. Furrer. Dordrecht: Kluwer Academic Publishers.
- Radaelli, P. G., Cox, D. E., Marezio, M., Cheong, S.-W., Schiffer, P. E. & Ramirez, A. P. (1995). *Phys. Rev. Lett.* **75**, 4488–4491.
- Schoenborn, B. P. & Knott, R. (1996). Editors. *Neutrons in Biology. Basic Life Sciences Series*, Vol. 64. New York: Plenum Press.
- Shull, C. G. & Smart, J. S. (1949). *Phys. Rev.* **76**, 1256–1257.
- Shull, C. G. & Yamada, Y. (1962). *J. Phys. Soc. Jpn*, **17**, Suppl. BIII, 1–6.
- Simpson, J. A., Cowley, R. A., McMorro, D. F., Ward, R. C. C., Wells, M. R., Carlile, C. J. & Adams, M. A. (1996). *J. Phys. Condens. Matter*, **8**, L187–L194.
- Soper, A. K., David, W. I. F., Sivia, D. S., Dennis, T. J. S., Hare, J. P. & Prassides, J. (1992). *Phys. Rev. B*, **4**, 6087–6094.
- Stokes, H. T., Decker, D. L., Nelson, H. M. & Jorgensen, J. D. (1993). *J. Phys. Condens. Matter*, **47**, 11082–11092.
- Willis, B. T. M. (1996). *International Tables for Crystallography*, Vol. B, pp. 384–391. Dordrecht: Kluwer Academic Publishers.
- Wollan, E. O. & Koehler, W. C. (1955). *Phys. Rev.* **100**, 545–563.
- Zheludev, A., Bonnet, M., Luneau, D., Ressouche, E., Rey, P. & Schweizer, J. (1995). *Physica (Utrecht)*, **B213**, 268–271.